3 Classical Model for a Microwave-Irradiated 2DEG in the Presence of Bichromatic Irradiation

The theoretical explanation [51, 50] of the recently observed zero resistance states [36, 37] in GaAs samples relies on the emergence of parameter regions with negative microscopic diagonal conductivity. The microscopic processes most likely responsible for negative conductivity – distribution function and displacement mechanisms – are inherently quantum mechanical. Any classical model with a parabolic electron dispersion only shows the conventional cyclotron resonance and does not show any further response to the microwave field due to Kohn's theorem [58]. Very interestingly, however, it can be shown that negative conductivity and, thus, zero resistance states can emerge from a classical Drude model driven by a microwave field, if one assumes the dispersion of the electrons to be weakly nonparabolic [59]. Due to the weak nonparabolicity of GaAs, this model is presumably irrelevant for the explanation of the present experiments, but could apply to other semiconductor systems with stronger nonparabolicity.

Most experiments on microwave-driven 2D electron systems carried out so far study the response of the system to a microwave field of a single, sharply defined, microwave frequency ω. Only very recently, the response to bichromatic irradiation was studied experimentally [38]. Our work concentrates on bichromatic irradiation, since interesting and qualitatively new effects arise in this situation. The most important parameter in bichromatically irradiated systems is the detuning between the two frequencies of the microwave field, i.e. the difference between the two distinct microwave frequencies applied. We will show in this chapter that, for weak detuning,[1] there is no qualitative difference between mono- and bichromatic irradiation, whereas for strong detuning, several novel effects arise, among which are the appearance of additional ZRS, parametric excitation of the cyclotron mode and multistability of the conductivity. We predict that the parametric resonance can translate into a dc current, which should be detectable in experiment. In addition, bichromatic irradiation experiments can be used to confirm that negative microscopic conductivity is indeed the origin of the ZRS. This test has recently been proposed and realized by Du and co-workers [38].

Parametric resonance in semiconductors has a long history: More than twenty years ago, Aronov *et al.* [60, 61, 62] proposed a way to parametrically excite the cyclotron mode of electrons in a magnetic field via a weak time modulation

[1] The detuning is "weak" in the sense that both frequencies are close to the cyclotron frequency ω_c and thereby close to each other.

of the amplitude of the dc magnetic field. The idea behind this proposal is that a modulation of the magnitude of the dc field with a frequency Ω translates into a corresponding modulation of the cyclotron frequency, so that the equation of motion of the electron reduces to that for a harmonic oscillator with a weakly time-modulated eigenfrequency. The solution of this equation is unstable, if the modulation frequency is close to $\Omega = 2\omega_c$. Unfortunately, this method of creating a parametric resonance in the electron system turns out to be technically unfeasible: For a characteristic magnetic field of $B = 0.1$ T, the cyclotron frequency is $\omega_c = 3.6 \cdot 10^{11}$ Hz, i.e. in the microwave range, so that conventional modulation of B with a frequency $2\omega_c$ is technically impossible. To bypass this obstacle, it was proposed in Ref. [62] to use microwave irradiation with frequency $2\omega_c$ to create a parametric resonance. The idea was that the *magnetic field* component of the pumping electromagnetic wave would provide the necessary oscillatory correction to the external magnetic field. In this chapter, we demonstrate that two nonresonant ac sources can *enforce* a parametric resonance of the type considered in Refs. [60, 61, 62] *without* any time modulation of the magnetic field. Remarkably, this bichromatic-radiation-induced cyclotron resonance emerges due to the nonparabolicity of the electron spectrum, which played the role of a stabilizing mechanism on the parametric resonance of Refs. [60, 61, 62].

In Section 3.1, we formulate the classical, single-electron Drude model for the two-dimensional electron gas irradiated by microwaves and show that negative contributions to the photocurrent can emerge in this model for nonparabolic band structures. If these negative contributions are large enough, they may result in a negative diagonal conductivity which may lead to microwave-induced zero resistance states (ZRS). Then, we extend these considerations to the bichromatic case and discuss the emergence of ZRS under bichromatic irradiation as well as the multistability of the conductivity for weak detuning of the two microwave frequencies in Section 3.2.1. Section 3.2.2 is devoted to the case of strong detuning and, mainly, to the parametric instability of the system. We also demonstrate the emergence of a dc current in the system under bichromatic irradiation and discuss a way to demonstrate the presence of negative diagonal conductivity. This chapter is based on Joas *et al.* [63].

3.1 Monochromatic Irradiation

The classical equation of motion of an electron in two dimensions, subjected to a perpendicular magnetic field $\mathbf{B}$, a dc electric field $\mathbf{E}$ and a monochromatic, linearly polarized microwave (ac) field $\mathcal{E}(t) = \mathcal{E}\cos(\omega t)$, as sketched in Fig. 3.1, is given by [59]

$$\frac{d\mathbf{p}}{dt} + \frac{\mathbf{p}}{\tau} - e(\mathbf{v} \times \mathbf{B}) = e\mathbf{E} + e\mathcal{E}\cos(\omega t) \quad , \tag{3.1}$$

where e is the electronic charge and $\mathbf{p}$ and $\mathbf{v}$ denote the electron momentum and velocity, respectively. A phenomenological relaxation time τ is included to account for disorder scattering.

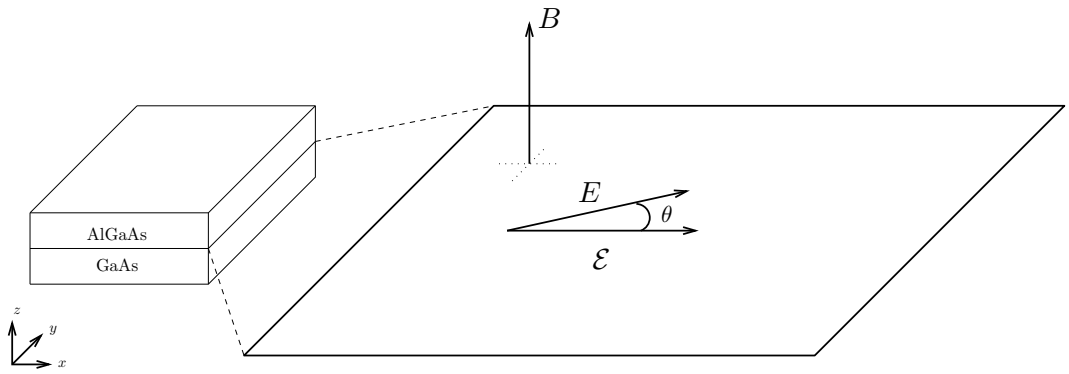

Figure 3.1: Sketch of the experimental setup and the relevant quantities in our model. The electron is confined to a two-dimensional plane and subject to a magnetic field B perpendicular to this plane, a small dc electric field E and an ac microwave field $\mathcal{E}$, which form an angle θ.

We assume a weakly nonparabolic electron dispersion

$$\varepsilon(p) = \frac{p^2}{2m}\left(1 - \frac{p^2}{2mE_0}\right) \quad , \tag{3.2}$$

where m is the electron mass and E_0 is an energy that typically is of the order of the bandgap. The strength of the nonparabolicity is given by the parameter $(mE_0)^{-1}$. Since the electron motion is confined to a two-dimensional plane, the momentum can be written as a complex number,

$$\mathcal{P} = p_x + ip_y \quad , \tag{3.3}$$

whose real and imaginary parts are the x- and y-components of momentum, respectively. The equation of motion can then be cast into the complex form

$$\frac{d\mathcal{P}}{dt} + \frac{\mathcal{P}}{\tau} - i\omega_c\mathcal{P} + \frac{i\omega_c}{mE_0}\mathcal{P}|\mathcal{P}|^2 = eEe^{i\theta} + \frac{e\mathcal{E}}{2}\left(e^{i\omega t} + e^{-i\omega t}\right) \quad , \tag{3.4}$$

where

$$\omega_c = \frac{eB}{m} \tag{3.5}$$

is the cyclotron frequency and θ is the angle between the polarization direction of the ac field and the dc field.

In principle, this equation of motion can be solved perturbatively to arbitrary order in the small nonparabolicity parameter $(mE_0)^{-1}$ using e.g. the Poincaré-Lindstedt perturbative expansion [64]. In the near-resonant case $\omega \simeq \omega_c$ and for high electron mobilities ($\omega_c\tau \gg 1$), however, it is sufficient to consider the following ansatz for the complex momentum

$$\mathcal{P}(t) = \mathcal{P}_0 + \mathcal{P}_+ \exp(i\omega t) + \mathcal{P}_- \exp(-i\omega t) \quad . \tag{3.6}$$

Near the cyclotron resonance, the absolute value of the resonant momentum component, $|\mathcal{P}_+|$, can be expected to be much larger than the absolute value of the nonresonant momentum component, $|\mathcal{P}_-|$, both being large in comparison

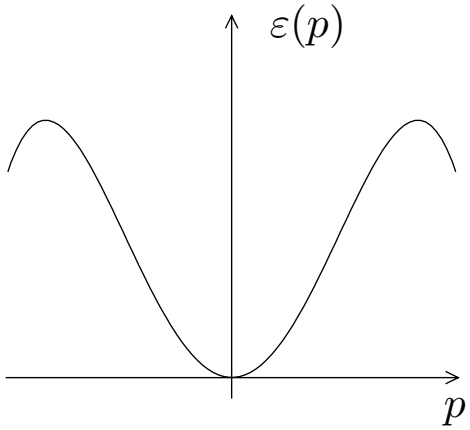

Figure 3.2: Exaggerated sketch of the nonparabolic electron dispersion $\varepsilon(p)$, Eq. (3.2).

to the absolute value of the small dc-component, $|\mathcal{P}_0|$, which is proportional to the weak applied dc field $|\mathbf{E}| = E$.

Substituting the ansatz, Eq. (3.6), into the equation of motion, Eq. (3.4), we find the following system of equations for the momentum components

$$\left[i(\omega-\omega_c)+\frac{1}{\tau}\right]\mathcal{P}_+ + \frac{i\omega_c}{mE_0}\mathcal{P}_+|\mathcal{P}_+|^2 = \frac{e\mathcal{E}}{2} \quad , \tag{3.7}$$

$$-i\left(\omega+\omega_c\right)\mathcal{P}_- = \frac{e\mathcal{E}}{2} \quad , \tag{3.8}$$

$$\left[\frac{1}{\tau} - i\omega_c\left(1-\frac{2|\mathcal{P}_+|^2}{mE_0}\right)\right]\mathcal{P}_0 + \left[\frac{2i\omega_c}{mE_0}\mathcal{P}_+\mathcal{P}_-\right]\mathcal{P}_0^* = eEe^{i\theta} \quad . \tag{3.9}$$

From Eq. (3.8), one immediately obtains for the nonresonant momentum component

$$\mathcal{P}_- = \frac{ie\mathcal{E}}{4\omega_c} \quad . \tag{3.10}$$

The solution of Eq. (3.7) can be formally presented as

$$\mathcal{P}_+ = \frac{e\mathcal{E}\tau}{2(1+i\Omega\tau)} \quad , \tag{3.11}$$

where

$$\Omega = \omega - \omega_c + \frac{\omega_c|\mathcal{P}_+|^2}{mE_0} \tag{3.12}$$

is the detuning of the microwave frequency from the cyclotron resonance, which is shifted away from ω_c due to irradiation.

Substituting $\mathcal{P}_+$ and $\mathcal{P}_-$ into Eq. (3.9), the longitudinal and transverse components of the drift momentum (with respect to the applied dc field) can be calculated from $\mathcal{P}_0$ to be

$$p_\parallel = \mathrm{Re}\left[\mathcal{P}_0 e^{-i\theta}\right] = \frac{eE}{\omega_c^2\tau}\left\{1 - \left[\frac{(e\mathcal{E}\tau)^2}{8mE_0}\right]\frac{\Omega\tau\sin(2\theta)-\cos(2\theta)}{1+(\Omega\tau)^2}\right\} \tag{3.13}$$

and

$$p_\perp = \mathrm{Im}\left[\mathcal{P}_0 e^{-i\theta}\right] = \frac{eE}{\omega_c}\left\{1 - \left[\frac{(e\mathcal{E})^2\tau}{8mE_0\omega_c}\right]\frac{\Omega\tau\cos(2\theta)+\sin(2\theta)}{1+(\Omega\tau)^2}\right\} \quad . \tag{3.14}$$

These momentum components are directly related to the conductivity components[2]

$$\sigma_d = \frac{ne^2}{m\omega_c}\left[\frac{1}{\omega_c\tau} - \left(\frac{\delta m}{2m}\right)\frac{\Omega\tau\sin(2\theta)-\cos(2\theta)}{\omega_c\tau}\right] \quad , \tag{3.15}$$

$$\sigma_t = \frac{ne^2}{m\omega_c}\left[1 - \left(\frac{\delta m}{2m}\right)\frac{\Omega\tau\cos(2\theta)+\sin(2\theta)}{\omega_c\tau}\right] \quad , \tag{3.16}$$

where n is the electron concentration and the irradiation-induced change of the effective mass

$$\frac{\delta m}{m} = \frac{|\mathcal{P}_+|^2}{mE_0} = \frac{(e\mathcal{E}\tau)^2}{4mE_0\left[1+(\Omega\tau)^2\right]} \tag{3.17}$$

is a measure for the intensity of the microwave field. Within a certain interval of magnetic fields near the cyclotron resonance, one is thus able to find negative diagonal conductivity, $\sigma_d < 0$, without a significant change of the Hall conductivity σ_t for specific relative orientations of the fields, if a number of conditions are fulfilled. The sign reversal of the conductivity occurs when the mobility is high, $\omega_c\tau \gg 1$, and when $\mathcal{E}$ is sufficiently strong, i.e. above some threshold value for the intensity of the microwave field. In the vicinity of the cyclotron resonance, σ_d turns negative even when the irradiation-induced change of the electron mass is relatively weak. The diagonal conductivity σ_d shows bistable hysteretic behavior as a function of the detuning from the cyclotron resonance for sufficiently large $\omega_c\tau$. For the case of monochromatic irradiation studied in this section, ZRS can thus emerge already on classical grounds, since absolute negative conductivity leads to an instability of the current pattern [51], as outlined in Chapter 2.

3.2 Bichromatic Irradiation

Denote by $\mathcal{E}_1$ and $\mathcal{E}_2$ the amplitudes of two linearly polarized ac fields[3] with frequencies ω_1 and ω_2, respectively. In the presence of a dc field E_{dc}, the equation of motion for the electron momentum $\mathcal{P} = p_x + ip_y$ takes the form

$$\begin{aligned}\frac{d\mathcal{P}}{dt} + \frac{\mathcal{P}}{\tau} - i\omega_c\mathcal{P} + \frac{i\omega_c}{mE_0}\mathcal{P}|\mathcal{P}|^2 = eE_{dc}e^{i\theta} + \frac{e\mathcal{E}_1}{2}\left(e^{i\omega_1 t} + e^{-i\omega_1 t}\right) \\ + \frac{e\mathcal{E}_2}{2}\left(e^{i\omega_2 t} + e^{-i\omega_2 t}\right) \quad ,\end{aligned} \tag{3.18}$$

[2] The elements of the resistivity tensor are connected to those of the conductivity tensor via $\rho_{xx} = \sigma_{xx}/(\sigma_{xx}^2 + \sigma_{xy}^2)$ and $\rho_{xy} = \sigma_{xy}/(\sigma_{xx}^2 + \sigma_{xy}^2)$. This means in particular that zero diagonal conductivity ensues zero diagonal resistivity – contrary to what one might naively expect.

[3] For a rotationally invariant spectrum, the effects discussed here require irradiation by linearly polarized ac fields. However, it is interesting to note that similar effects would be expected even for circularly polarized ac fields if the nonparabolicity is not rotationally invariant, such as $p_x^4 + p_y^4$. This may be relevant for the hole bands in GaAs.

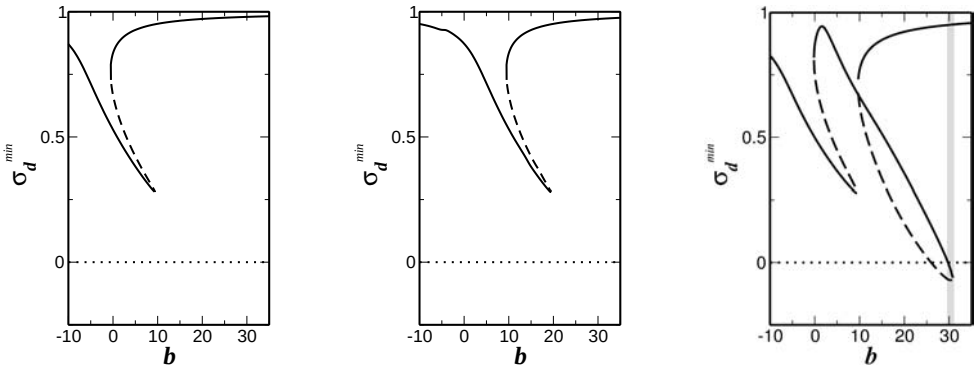

Figure 3.3: Dimensionless diagonal conductivity (in units of the Drude conductivity) plotted from Eq. (3.30) versus the dimensionless magnetic field, defined by Eq. (3.31), for three cases: (a) *monochromatic* irradiation with frequency ω_1 and dimensionless intensity $A = 14.4$; (b) *monochromatic* irradiation with the same intensity as in (a) and frequency $\omega_2 = 5\omega_1/3$; (c) *bichromatic* case: response to simultaneous irradiation with two microwave sources having the same intensities and frequencies as in (a) and (b). The emerging region of negative diagonal conductivity is shaded in gray. All three plots (a)-(c) have been calculated for $(\omega_1 + \omega_2)\,\tau/2 = 20$. Full and dashed lines correspond to stable and unstable branches, respectively.

where ω_c is the cyclotron frequency, τ is the relaxation time, and θ is the orientation of the weak dc field with respect to the fields $\mathcal{E}_1$, $\mathcal{E}_2$, which we assume to be parallel to each other. For a monochromatic ac drive, $\mathcal{E}_2 = 0$, it was demonstrated in Section 3.1 that within a certain interval of magnetic fields near the cyclotron resonance, Eq. (3.18) implies negative diagonal conductivity, $\sigma_d < 0$, without significant change of the Hall conductivity. This sign reversal occurs when the mobility is high, $\omega_c\tau \gg 1$, and $\mathcal{E}_1$ is sufficiently strong. In the vicinity of the cyclotron resonance, σ_d turns negative even when the irradiation-induced change of the electron mass is relatively weak. Thus, the simple model Eq. (3.18) exhibits negative photoconductivity without invoking Landau quantization. It also predicts bistable hysteretic behavior of σ_d as a function of the detuning from the cyclotron resonance for sufficiently large $\omega_c\tau$.

We now extend these considerations to the bichromatic case. The most convincing illustration that the response to irradiation by two ac fields cannot simply be reduced to the superposition of the responses to each individual field, is presented in Fig. 3.3. It is seen in Figs. 3.3(a,b) that the individual fields of equal intensity and frequency ratio 5 : 3 are unable to reverse the sign of the diagonal conductivity at any magnetic field. At the same time, upon *simultaneous* irradiation by both fields, a domain of magnetic fields emerges, within which the diagonal conductivity is negative (see Fig. 3.3(c)).

In addition, our study reveals the following new features that are specific to the bichromatic case:

(*i*) The presence of the second ac field on the right-hand side of Eq. (3.18)

gives rise to a second domain of magnetic field, within which σ_d is negative. Upon increasing the intensities of the two ac fields, the two domains of negative photoconductivity merge into a single domain which broadens much faster with the ac intensity than in the monochromatic case.
(*ii*) For monochromatic irradiation, σ_d could assume either one or two stable values. By contrast, under bichromatic irradiation, we find a *multistable* regime within certain domains of magnetic field.
(*iii*) In the vicinity of the conditions $(\omega_1 + \omega_2) = 2\omega_c$ and $|\omega_1 - \omega_2| = 2\omega_c$, a nonparabolicity-induced *parametric* instability develops in the system. As a result of this instability, the components $(\omega_1 + \omega_2)/2$ and $|\omega_1 - \omega_2|/2$ emerge in addition to the conventional frequencies ω_1 and ω_2 of the momentum oscillations. These components, upon mixing with the components ω_1, ω_2, give rise to components of $\mathcal{P}$ oscillating with frequencies $3\omega_1 - \omega_2$. Thus, for *bichromatic* irradiation, two high-frequency ac driving fields can create a low frequency current circulating in the system. In particular, for $\omega_2 = 3\omega_1 \simeq 3\omega_c/2$ the system exhibits a dc response to the ac drive.

The importance of the nonparabolicity in experiment can be estimated by studying the dimensionless quantity $(e\mathcal{E}\tau)^2 / (mE_0)$, where $\mathcal{E}$ is the amplitude of the microwave electric field. Assuming sample dimensions of 10^{-2} cm and a microwave power of 100 μW, taken from Ref. [37], the microwave electric field is of the order of $\mathcal{E} \sim 1$ V/cm. For the experimental mobility $\mu = 2.5 \times 10^7$ cm^2/Vs and for a nonparabolicity parameter $E_0 = 1$ eV, this yields a value of $(e\mathcal{E}\tau)^2 / (mE_0) \simeq 0.03$ (this estimate may be too optimistic for the conduction band of GaAs). In the monochromatic case, negative σ_d is achieved for $(e\mathcal{E}\tau)^2 / (mE_0) \gtrsim (\omega_c\tau)^{-1}$, which is compatible with the value $\omega_c\tau \sim 50$ from Ref. [37]. This agreement can be reached in spite of the smallness of the nonparabolicity, since the latter is compensated by the long scattering time in the ultrahigh mobility samples studied [37, 36]. One can also estimate that for the same parameters, the energy $(e\mathcal{E}\tau)^2/(2m)$ absorbed by an electron during the relaxation time τ exceeds the Landau-level spacing $\hbar\omega_c$. Under this condition, one expects the classical description to be appropriate.

3.2.1 Weak Detuning

For monochromatic irradiation, the cyclotron resonance develops when the microwave frequency is close to the cyclotron frequency ω_c. In this section, we consider bichromatic irradiation when both frequencies ω_1 and ω_2 are close to ω_c, $|\omega_1 - \omega_c| \ll \omega_c$ and $|\omega_2 - \omega_c| \ll \omega_c$, so that the cyclotron resonances due to ω_1 and ω_2 can interfere with each other.

Calculation of the Diagonal Conductivity

In analogy to Ref. [59], we search for solutions of Eq. (3.18) in the form

$$\begin{aligned}\mathcal{P}(t) = \mathcal{P}_0 + \mathcal{P}_1^+ \exp(i\omega_1 t) + \mathcal{P}_1^- \exp(-i\omega_1 t) \\ + \mathcal{P}_2^+ \exp(i\omega_2 t) + \mathcal{P}_2^- \exp(-i\omega_2 t) \quad ,\end{aligned} \tag{3.19}$$

where $\mathcal{P}_0$ is a small dc component proportional to E_{dc}. The momentum components $\mathcal{P}_1^-$ and $\mathcal{P}_2^-$ are nonresonant and can be found from the simplified equations

$$-i(\omega_1+\omega_c)\mathcal{P}_1^- = \frac{e\mathcal{E}_1}{2} \quad , \tag{3.20}$$

$$-i(\omega_2+\omega_c)\mathcal{P}_2^- = \frac{e\mathcal{E}_2}{2} \quad , \tag{3.21}$$

where we neglect both relaxation and nonlinearity. However, relaxation and nonlinearity must be taken into account when calculating the resonant momentum components $\mathcal{P}_1^+$ and $\mathcal{P}_2^+$. Substituting Eq. (3.19) into Eq. (3.18) and taking into account that $|\mathcal{P}_1^-|, |\mathcal{P}_2^-| \ll |\mathcal{P}_1^+|, |\mathcal{P}_2^+|$, we arrive at a system of coupled equations for the resonant momentum components,

$$\left[i\left(\omega_1-\omega_c\right)+\frac{1}{\tau}+\frac{i\omega_c}{mE_0}\left(|\mathcal{P}_1^+|^2+2|\mathcal{P}_2^+|^2\right)\right]\mathcal{P}_1^+ = \frac{e\mathcal{E}_1}{2} \quad , \tag{3.22}$$

$$\left[i\left(\omega_2-\omega_c\right)+\frac{1}{\tau}+\frac{i\omega_c}{mE_0}\left(2|\mathcal{P}_1^+|^2+|\mathcal{P}_2^+|^2\right)\right]\mathcal{P}_2^+ = \frac{e\mathcal{E}_2}{2} \quad . \tag{3.23}$$

Despite the inequalities $|\mathcal{P}_1^+| \ll |\mathcal{P}_1^-|$ and $|\mathcal{P}_2^+| \ll |\mathcal{P}_2^-|$, it is crucial not to neglect the nonresonant components $\mathcal{P}_1^-$ and $\mathcal{P}_2^-$ when considering the dc component $\mathcal{P}_0$. This yields

$$\begin{aligned}\left[-i\omega_c+\frac{1}{\tau}+\frac{2i\omega_c}{mE_0}\left(|\mathcal{P}_1^+|^2+|\mathcal{P}_2^+|^2\right)\right]\mathcal{P}_0 & \\ +\frac{2i\omega_c}{mE_0}\left[\mathcal{P}_1^+\mathcal{P}_1^-+\mathcal{P}_2^+\mathcal{P}_2^-\right]\mathcal{P}_0^* &= eE_{dc}e^{i\theta}.\end{aligned} \tag{3.24}$$

Due to the nonlinearity, the microwave intensities induce an effective shift in the resonance frequency ω_c. Thus, it is convenient to introduce effective detunings Ω_1 and Ω_2 by

$$\Omega_1 = \omega_1-\omega_c+\frac{\omega_c}{mE_0}\left(|\mathcal{P}_1^+|^2+2|\mathcal{P}_2^+|^2\right) \quad , \tag{3.25}$$

$$\Omega_2 = \omega_2-\omega_c+\frac{\omega_c}{mE_0}\left(2|\mathcal{P}_1^+|^2+|\mathcal{P}_2^+|^2\right) \quad , \tag{3.26}$$

and to present formal solutions of Eqs. (3.22-3.23) in the form

$$\mathcal{P}_1^+ = \frac{e\mathcal{E}_1\tau}{2\left(1+i\Omega_1\tau\right)} \quad , \qquad \mathcal{P}_2^+ = \frac{e\mathcal{E}_2\tau}{2\left(1+i\Omega_2\tau\right)} \quad . \tag{3.27}$$

Note that the detunings Ω_1 and Ω_2 themselves depend on $\mathcal{P}_1^+$ and $\mathcal{P}_2^+$, so that Eqs. (3.25-3.27) should be considered as a system of nonlinear equations for the resonant momentum components $\mathcal{P}_1^+$ and $\mathcal{P}_2^+$. Assuming that the detunings Ω_1 and Ω_2 are known, the solution of Eq. (3.24) yields for the dc component

$$\mathcal{P}_0 = \frac{eE_{dc}}{\omega_c^2\tau}\left\{\left(1+i\omega_c\tau\right)e^{i\theta}+\frac{1}{4mE_0}\left[\frac{\left(e\mathcal{E}_1\tau\right)^2}{1+i\Omega_1\tau}+\frac{\left(e\mathcal{E}_2\tau\right)^2}{1+i\Omega_2\tau}\right]e^{-i\theta}\right\} \quad . \tag{3.28}$$

The diagonal conductivity σ_d is proportional to $\mathrm{Re}\left[\mathcal{P}_0 e^{-i\theta}\right]$. Thus, the second term in Eq. (3.28) gives rise to a θ-dependence of the nonparabolicity-induced contribution to the diagonal conductivity which is given by $\sin(2\theta - \phi)$. Here, ϕ satisfies the equation

$$\tan\phi = \frac{\Omega_1\tau\left(1+\Omega_2^2\tau^2\right)\mathcal{E}_1^2 + \Omega_2\tau\left(1+\Omega_1^2\tau^2\right)\mathcal{E}_2^2}{\left(1+\Omega_2^2\tau^2\right)\mathcal{E}_1^2 + \left(1+\Omega_1^2\tau^2\right)\mathcal{E}_2^2} \quad . \tag{3.29}$$

We deduce that the minimal value of σ_d is given by

$$\sigma_d^{min} = \frac{ne^2}{m\omega_c^2\tau}\left\{1 - \frac{e^2\tau^2}{4mE_0}\left[\frac{\left(\mathcal{E}_1^2\Omega_2\tau + \mathcal{E}_2^2\Omega_1\tau\right)^2 + \left(\mathcal{E}_1^2 + \mathcal{E}_2^2\right)^2}{\left(1+\Omega_1^2\tau^2\right)\left(1+\Omega_2^2\tau^2\right)}\right]^{1/2}\right\} \quad . \tag{3.30}$$

In the following, we will be particularly interested in σ_d^{min}, since the condition $\sigma_d^{min} < 0$ is sufficient for the formation of the zero-resistance state.

Numerical Results: Multistability

As demonstrated in Ref. [59], the diagonal conductivity in the monochromatic case shows a region of bistability. In the bichromatic case under study, even multistable behavior may emerge, as will now be shown. We measure the frequency difference of the ac fields by $\Delta = (\omega_1 - \omega_2)\,\tau$ and the magnetic field by

$$b = \left(\omega_c - \frac{\omega_1+\omega_2}{2}\right)\tau \quad , \tag{3.31}$$

which depends linearly on the magnetic field B. Upon substituting the formal solutions $\mathcal{P}_1^+$ and $\mathcal{P}_2^+$ of Eq. (3.27) into Eqs. (3.25-3.26), these can be written as a pair of coupled equations for the effective detunings $\Omega_1\tau$ and $\Omega_2\tau$

$$\Omega_1\tau = \frac{\Delta}{2} - b + A\left[\frac{1}{1+(\Omega_1\tau)^2} + \frac{2\eta^2}{1+(\Omega_2\tau)^2}\right] \quad , \tag{3.32}$$

$$\Omega_2\tau = -\frac{\Delta}{2} - b + A\left[\frac{2}{1+(\Omega_1\tau)^2} + \frac{\eta^2}{1+(\Omega_2\tau)^2}\right] \quad , \tag{3.33}$$

where η and A, given by

$$\eta = \mathcal{E}_2/\mathcal{E}_1 \quad , \qquad A = \omega_c\tau\frac{(e\mathcal{E}_1\tau)^2}{4mE_0} \quad , \tag{3.34}$$

measure the ratio of the field amplitudes and the ratio of the absolute field intensities to the nonparabolicity of the electron spectrum, respectively. As in the monochromatic case, the strength of the first order correction to the Drude conductivity is proportional to the microwave intensity and thus to A. At fixed magnetic field b and fixed ac frequencies and amplitudes, this coupled system of two third-order equations can yield up to nine simultaneous solutions

$(\Omega_1\tau, \Omega_2\tau)$ for the effective detunings. Since σ_d^{min} is directly related to these effective detunings via

$$\sigma_d^{min} = \sigma_D \Bigg\{ 1 - \frac{A}{\omega_c\tau} \Bigg[\frac{1}{1+(\Omega_1\tau)^2} + \frac{\eta^4}{1+(\Omega_2\tau)^2} + \frac{2\eta^2\left(1+\Omega_1\tau\Omega_2\tau\right)}{\left(1+(\Omega_1\tau)^2\right)\left(1+(\Omega_2\tau)^2\right)} \Bigg]^{1/2} \Bigg\} \quad , \tag{3.35}$$

where $\sigma_D = ne^2/(\omega_c^2\tau)$ is the Drude conductivity, there are up to nine individual branches of σ_d^{min} at any given b. This multistable behavior occurs in the vicinity of the resonance and will be studied below for the specific case of $\eta = 1$ (i.e., equal field amplitudes).

We first focus on the dependence of $\sigma_d^{min}(b)$ on Δ. For large Δ, i.e. markedly different ac frequencies, we expect two separate regions in b where σ_d^{min} deviates significantly from the Drude result. These are the regions where the cyclotron frequency is in resonance with one of the two ac frequencies, i.e. either $\omega_1 \simeq \omega_c$ or $\omega_2 \simeq \omega_c$. Inside these regions, the behavior with respect to b is very similar to the monochromatic case, except that the irradiation-induced effective shift of ω_c now depends on both external frequencies. In particular, the emergence of bistable regions inside these two separate intervals is to be expected, in close analogy to the monochromatic case. This can be seen in Fig. 3.4 (top), where σ_d^{min} is shown as a function of magnetic field b for rather large Δ. Two dips in σ_d^{min} can be clearly discerned, the inner branches of which are unstable. Upon reducing Δ, the two dips move closer together up to a point where the frequencies ω_1 and ω_2 are so close that the analogy to the monochromatic case breaks down and the two dips start to interact to finally form a single multistable dip in the limit $\Delta \to 0$. This behavior is exemplified in Fig. 3.4 (middle and bottom). It can be seen that multiple solutions of $\sigma_d^{min}(b)$ develop upon reducing Δ.

Next, we consider the case of negative diagonal conductivity and study the evolution of $\sigma_d^{min}(b)$ with magnetic field b. As expected, there is a threshold intensity below which no negative diagonal conductivity is observed. Upon increasing the field amplitudes and thus A, the negative first order correction to the Drude conductivity grows linearly with $A/(\omega_c\tau)$ as can be seen from Eq. (3.35). When this correction exceeds unity, negative σ_d^{min} is to be expected in some regions of magnetic field b. Fig. 3.5 shows $\sigma_d^{min}(b)$ for three specific values of A. It can be seen that at low A, no regions in b with negative diagonal conductivity can be observed. At higher A, two regions in b show negative σ_d^{min}-branches as is also indicated by the shaded regions in Fig. 3.5(b). For even higher A, a single large region in b shows negative diagonal conductivity.

To clarify the evolution of these regions with increasing field amplitudes, we plotted the extension of the regions in b as a function of A. The result is shown in Fig. 3.6. It is remarkable that above the threshold value of A, first a single region appears that shows negative σ_d^{min}. Then, in the immediate vicinity of the threshold a second, well separated region develops. Upon further increasing A, the width of these regions grows and, eventually, the two regions merge to

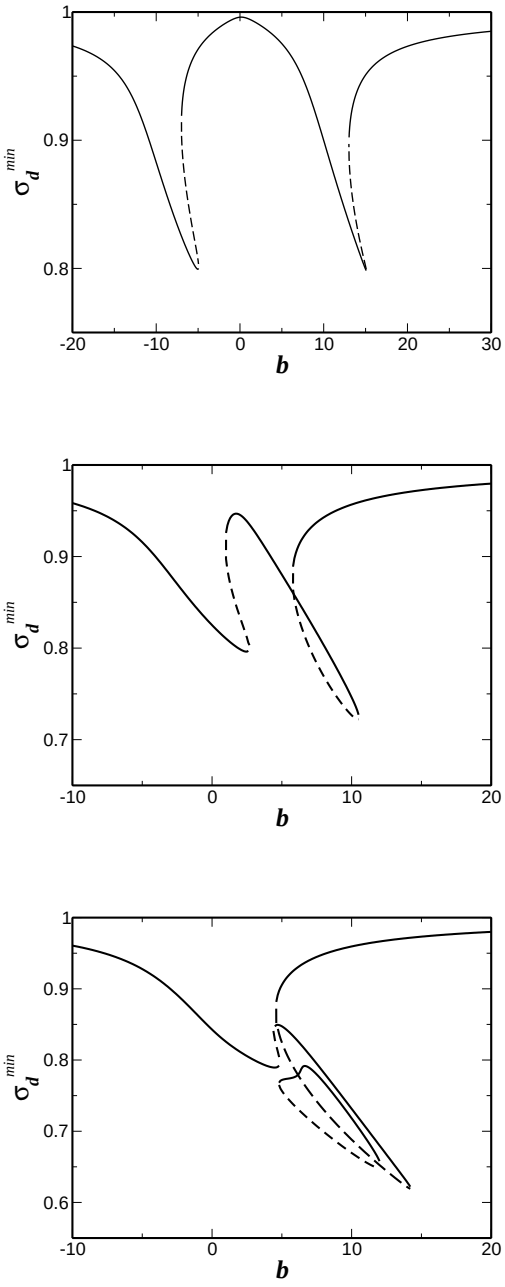

Figure 3.4: Evolution of the dimensionless minimal conductivity σ_d^{min} (in units of the Drude conductivity σ_D) as a function of magnetic field b, defined in Eq. (3.31), for three different values of Δ: $\Delta = 20$ (top), $\Delta = 5$ (middle), $\Delta = 1$ (bottom). The curves have been calculated for the values of parameters $\eta = 1$, $A = 5$ (defined by Eq. (3.34)), and $\omega_c\tau = 25$. The distance of the two dips that can be clearly discerned in the topmost figure is roughly Δ. When lowering Δ, the dips move closer together (middle figure) and finally merge (bottom figure). In addition, multistable regions emerge. As in Fig. 3.3, unstable branches are plotted as dashed lines.

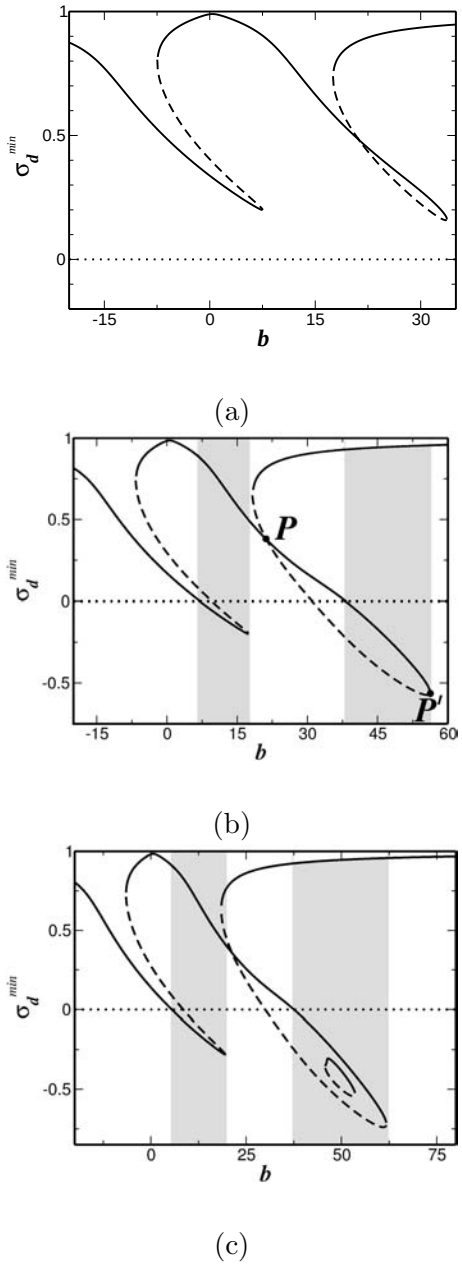

Figure 3.5: The dimensionless minimal diagonal conductivity, $\sigma_d^{min}(b)$, defined by Eq. (3.35), plotted for three different values of the dimensionless intensity A of the two ac fields: (a) $A = 20$, (b) $A = 30$, (c) $A = 32$. The domains of magnetic field b with negative σ_d^{min} are shaded. The dotted line indicates the boundary between positive and negative σ_d^{min}. Unstable branches are dashed. The curves have been calculated for the values of the parameters $\eta = 1$, $\Delta = (\omega_1 - \omega_2)\tau = 25$ and $\omega_c\tau = 25$. In (b), the point **P** is a point where a continuous stable and a continuous unstable branch intersect without "noticing" each other, while the point $\mathbf{P}'$ is a cusp which separates a stable from an unstable branch.

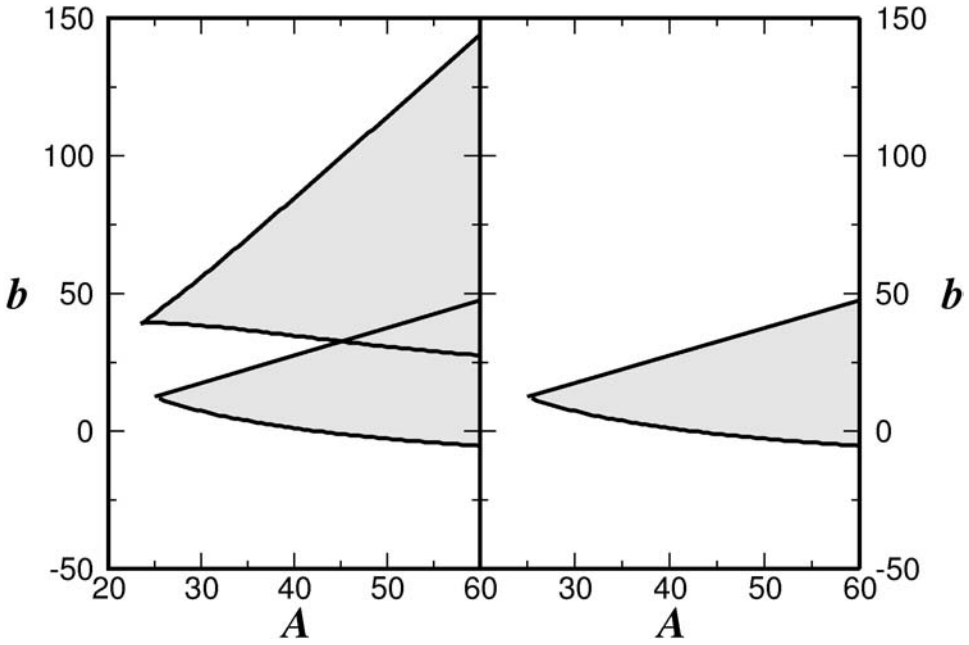

Figure 3.6: Evolution of the regions of negative σ_d^{min} with irradiation intensity, A. Shown are the bichromatic case (left panel) and the monochromatic case (right panel). In both cases, only the dominant (stable) branches are shown to avoid confusion. The parameters are the same as in Fig. 3.5.

form a single broad region of negative diagonal conductivity. For comparison, we also show the monochromatic case in the right hand panel of Fig. 3.6.

Stability of Different Branches

The stability of the various branches of $\sigma_d^{min}(b)$ as shown by solid and dashed lines in Figs. 3.3-3.5, can be obtained from standard stability analysis [65]. As usual, we find that stable and unstable branches "meet" at cusps, as clearly seen at the minima of $\sigma_d^{min}(b)$ in Figs. 3.3 and 3.4. The transitions from unstable to stable branches at larger b in these figures are also accompanied by cusps, although this can not necessarily be discerned within the resolution of the figures. The number of branches increases with the irradiation intensity (see Figs. 3.4 and 3.5). The basic rule that stable and unstable branches meet in cusps remains valid, although this statement becomes less trivial. For example, in Fig. 3.5(b), stable and unstable branches intersect at point **P** without "noticing each other". Accordingly, there is no cusp at this point. At the same time, there is a cusp at $\mathbf{P}'$ in Fig. 3.5(b) where the same branches switch between stable and unstable. Figs. 3.4 (bottom) and 3.5(c) illustrate how new branches and multistability emerge with increasing irradiation intensity. The emergence of new stable and unstable branches occurs in pairs which meet at additional cusps. In both Figures 3.4 (bottom) and 3.5(c), there are regions in magnetic field with three coexisting stable solutions (tristability). Further increase of A

would lead to up to eight cusps in Fig. 3.5(c), each of which is a meeting point of stable and unstable branches. Thus, the tristability situation illustrated in Fig. 3.5(c) will evolve into a magnetic field domain with "four-stability".

3.2.2 Strong Detuning

In this section, we consider the case when both frequencies ω_1 and ω_2 are tuned away from ω_c. This implies that the system of coupled equations for the resonant momentum components, Eqs. (3.22-3.23), decouples and acquires the obvious solutions

$$\mathcal{P}_1^+ = \frac{e\mathcal{E}_1\tau}{2\left[1+i\left(\omega_1-\omega_c\right)\tau\right]} \quad , \qquad \mathcal{P}_2^+ = \frac{e\mathcal{E}_2\tau}{2\left[1+i\left(\omega_2-\omega_c\right)\tau\right]} \quad . \tag{3.36}$$

The condition $e\mathcal{E}_1$, $e\mathcal{E}_2 \ll \omega_c\left(mE_0\right)^{1/2}$ for decoupling follows from Eqs. (3.22-3.23), assuming that $|\omega_1-\omega_c|$, $|\omega_2-\omega_c| \sim \omega_c \gg 1/\tau$. Interestingly, even under this condition, the solutions are unstable for certain relations between the frequencies ω_1, ω_2. The mechanism for this instability consists of nonparabolicity-induced mixing of the two external drive frequencies, which results in a modulation of the effective cyclotron frequency. This modulation, in turn, can lead to *parametric* resonance.

To perform the stability analysis of the solutions Eq. (3.36), we introduce a small deviation $\mathcal{P} \to \mathcal{P} + \delta\mathcal{P}$ and linearize Eq. (3.18) with respect to $\delta\mathcal{P}$. This yields

$$\frac{d}{dt}\left(\delta\mathcal{P}\right) + \left(\frac{1}{\tau} - i\omega_c + \frac{2i\omega_c}{mE_0}|\mathcal{P}|^2\right)\delta\mathcal{P} + \frac{i\omega_c}{mE_0}\mathcal{P}^2\left(\delta\mathcal{P}\right)^* = 0 \quad . \tag{3.37}$$

This equation couples $\delta\mathcal{P}$ to $(\delta\mathcal{P})^*$ via the nonparabolicity of the electron spectrum. The corresponding equation for $\delta\mathcal{P}^*$ reads

$$\frac{d}{dt}\left(\delta\mathcal{P}^*\right) + \left(\frac{1}{\tau} + i\omega_c - \frac{2i\omega_c}{mE_0}|\mathcal{P}|^2\right)\delta\mathcal{P}^* - \frac{i\omega_c}{mE_0}\left(\mathcal{P}^*\right)^2\delta\mathcal{P} = 0 \quad . \tag{3.38}$$

As can be seen from Eq. (3.19), the coupling coefficient $\mathcal{P}^2$ contains the harmonics $\pm 2\omega_1$, $\pm 2\omega_2$, $\pm(\omega_1+\omega_2)$, and $\pm(\omega_1-\omega_2)$. This suggests that $\delta\mathcal{P}(t)$ also contains a number of harmonics, namely, $\pm\omega_1$, $\pm\omega_2$, $\pm(\omega_1+\omega_2)/2$, and $\pm(\omega_1-\omega_2)/2$. An instability might develop when either one of these frequencies is close to ω_c. Thus, in the monochromatic case, the instability develops only in the vicinity of the cyclotron resonance $\omega_1 \simeq \omega_c$. The branches denoted by dashed lines in Figs. 3.3(a,b) are unstable due to this instability. By contrast, the bichromatic case offers two additional options for an instability to develop, even if the frequencies ω_1, ω_2 are nonresonant, namely $\omega_c \simeq \left(\omega_1+\omega_2\right)/2$ and $\omega_c \simeq |\left(\omega_1-\omega_2\right)|/2$. Both cases can be treated in a similar way. Therefore, we mainly focus on the first case below.

Parametric Instability at $(\omega_1 + \omega_2) \simeq 2\omega_c$

Upon substituting the ansatz

$$\begin{aligned} \delta\mathcal{P}(t) &= C \exp\left\{\left[\Gamma + \frac{i\,(\omega_1+\omega_2)}{2}\right] t\right\} \quad , \\ \delta\mathcal{P}(t)^* &= C^* \exp\left\{\left[\Gamma - \frac{i\,(\omega_1+\omega_2)}{2}\right] t\right\} \end{aligned} \tag{3.39}$$

into Eqs. (3.37-3.38) and keeping only resonant terms, we obtain the following system of equations for C and C^*

$$\left[\Gamma + \frac{1}{\tau} + \frac{i\,(\omega_1+\omega_2-2\omega_c)}{2} + \frac{2i\omega_c}{mE_0}\left(|\mathcal{P}_1^+|^2 + |\mathcal{P}_2^+|^2\right)\right] C = -\frac{2i\omega_c}{mE_0}\mathcal{P}_1^+\mathcal{P}_2^+ C^* \quad , \tag{3.40}$$

$$\left[\Gamma + \frac{1}{\tau} - \frac{i\,(\omega_1+\omega_2-2\omega_c)}{2} - \frac{2i\omega_c}{mE_0}\left(|\mathcal{P}_1^+|^2 + |\mathcal{P}_2^+|^2\right)\right] C^* = \frac{2i\omega_c}{mE_0}\left(\mathcal{P}_1^+\mathcal{P}_2^+\right)^* C \quad . \tag{3.41}$$

The most favorable condition for instability consequently is determined by the relation

$$\begin{aligned} \omega_1 + \omega_2 &= 2\omega_c\left[1 - \frac{2}{mE_0}\left(|\mathcal{P}_1^+|^2 + |\mathcal{P}_2^+|^2\right)\right] \\ &\simeq 2\omega_c\left\{1 - \frac{e^2}{2mE_0}\left[\frac{\mathcal{E}_1^2}{(\omega_1-\omega_c)^2} + \frac{\mathcal{E}_2^2}{(\omega_2-\omega_c)^2}\right]\right\} \\ &\simeq 2\omega_c\left[1 - \frac{2e^2\left(\mathcal{E}_1^2+\mathcal{E}_2^2\right)}{mE_0\,(\omega_1-\omega_2)^2}\right] \quad , \end{aligned} \tag{3.42}$$

where Eq. (3.36) has been used. If ω_1 and ω_2 fulfill this relation, the increment Γ is maximal and takes on the value

$$\begin{aligned} \Gamma_{max} &= -\frac{1}{\tau} + \left(\frac{2\omega_c}{mE_0}\right)|\mathcal{P}_1^+\mathcal{P}_2^+| \\ &\simeq -\frac{1}{\tau} + \left|\frac{e^2\omega_c\mathcal{E}_1\mathcal{E}_2}{mE_0\,(\omega_1-\omega_c)\,(\omega_2-\omega_c)}\right| \\ &\simeq -\frac{1}{\tau} + \frac{e^2\,(\omega_1+\omega_2)\,|\mathcal{E}_1\mathcal{E}_2|}{mE_0\,(\omega_1-\omega_2)^2} \quad . \end{aligned} \tag{3.43}$$

The parametric instability develops if Γ_{max} is positive. It is important to note that the condition $\Gamma_{max} > 0$ is consistent with the condition of strong detuning when the simplified expressions, Eq. (3.36), are valid. Indeed, assuming $|\omega_1 - \omega_c| \sim |\omega_2 - \omega_c| \sim \omega_c$, the two conditions can be presented as $\omega_c\,(mE_0)^{1/2} \gg e\mathcal{E}_1, e\mathcal{E}_2 \gg \tau^{-1}\,(mE_0)^{1/2}$. Therefore, for $\omega_c\tau \gg 1$, there exists an interval of the amplitudes of the ac fields within which both conditions are met. Note also

that the parametric resonance does not develop exactly at $\omega_c = (\omega_1 + \omega_2)/2$, i.e. at $b = 0$. In fact, from Eqs. (3.42-3.43) it can be concluded that $\Gamma_{max} > 0$ corresponds to $b \gtrsim 1$. In experimental situations, when ω_1 and ω_2 are fixed, Eq. (3.42) can also be viewed as a condition for the magnetic field $\omega_c = \omega_c^{opt}$ at which the parametric instability is most pronounced. The interval of ω_c around ω_c^{opt} within which the increment assumes positive values can be found from the dependence $\Gamma(\omega_c)$ given by

$$\begin{aligned} \Gamma(\omega_c) &= -\frac{1}{\tau} + \sqrt{\left(\Gamma_{max} + \frac{1}{\tau}\right)^2 - \left(\omega_c - \omega_c^{opt}\right)^2} \\ &\simeq -\frac{1}{\tau} + \sqrt{\left[\frac{e^2\left(\omega_1+\omega_2\right)|\mathcal{E}_1\mathcal{E}_2|}{mE_0\left(\omega_1-\omega_2\right)^2}\right]^2 - \left(\omega_c - \omega_c^{opt}\right)^2} \quad . \end{aligned} \tag{3.44}$$

Upon setting $\Gamma(\omega_c) = 0$ in the left-hand side of Eq. (3.44), we find the width of the interval to be

$$\begin{aligned} |\omega_c - \omega_c^{opt}| &\leq \left\{\left[\frac{e^2\omega_c|\mathcal{E}_1\mathcal{E}_2|}{2mE_0\left(\omega_1-\omega_c\right)^2}\right]^2 - \frac{1}{\tau^2}\right\}^{1/2} \\ &\simeq \left\{\left[\frac{e^2\left(\omega_1+\omega_2\right)|\mathcal{E}_1\mathcal{E}_2|}{mE_0\left(\omega_1-\omega_2\right)^2}\right]^2 - \frac{1}{\tau^2}\right\}^{1/2} \quad . \end{aligned} \tag{3.45}$$

It is instructive to reformulate the condition for the parametric instability in a different way. Assume for simplicity that $\mathcal{E}_1 = \mathcal{E}_2$. Then the combination $e^2|\mathcal{E}_1\mathcal{E}_2|/2mE_0(\omega_1 - \omega_c)^2$ is equal to $\delta m/m$, where $\delta m/m$ is the relative correction to the electron effective mass due to irradiation (see Section 3.1). From Eq. (3.43) it follows that the condition $\Gamma_{max} > 0$ can be presented as $(\omega_c\tau)(\delta m/m) > 1$. With $\omega_c\tau \gg 1$ this condition can be satisfied even for $\delta m \ll m$. Note that in the case of weak detuning, the same condition is required for the dc conductivity to assume negative values near the cyclotron resonance.

Summarizing, we arrive at the following scenario: In the case of strong detuning, there is no mutual influence of the responses to the ac fields $\mathcal{E}_1$ and $\mathcal{E}_2$ as long as they are weak. However, as the product $|\mathcal{E}_1\mathcal{E}_2|$ increases and reaches a critical value $|\mathcal{E}_1\mathcal{E}_2|_c$, the threshold, $\Gamma_{max} = 0$, where Γ_{max} is given by Eq. (3.43), is exceeded at the magnetic field $\omega_c = \omega_c^{opt}$ determined by Eq. (3.42). Above the threshold, fluctuations with frequencies close to $(\omega_1 + \omega_2)/2$ are amplified. This parametric instability is solely due to the nonparabolicity. Then the natural question arises: At which level above the threshold does the momentum component of frequency $(\omega_1 + \omega_2)/2$ saturate? This question will be addressed below.

Parametric Instability at $|\omega_1 - \omega_2| \simeq 2\omega_c$

We now briefly discuss the parametric instability at weak magnetic fields $\omega_c \simeq |(\omega_1 - \omega_2)|/2$. Without loss of generality, we assume $\omega_1 > \omega_2$. In this case, the

optimal magnetic field $\tilde{\omega}_c^{opt}$ is smaller than in the previous case and reads

$$\begin{aligned}\omega_1 - \omega_2 &\simeq 2\tilde{\omega}_c^{opt}\left\{1 - \frac{e^2}{2mE_0}\left[\frac{\mathcal{E}_1^2}{\left(\omega_1 - \tilde{\omega}_c^{opt}\right)^2} + \frac{\mathcal{E}_2^2}{\left(\omega_2 - \tilde{\omega}_c^{opt}\right)^2}\right]\right\} \\ &\simeq 2\tilde{\omega}_c^{opt}\left\{1 - \frac{2e^2}{mE_0}\left[\frac{\mathcal{E}_1^2}{(\omega_1+\omega_2)^2} + \frac{\mathcal{E}_2^2}{(3\omega_2-\omega_1)^2}\right]\right\} \quad . \end{aligned} \tag{3.46}$$

At $\omega_c = \tilde{\omega}_c^{opt}$, the threshold condition for parametric instability, analogous to Eq. (3.43), has the form

$$\tilde{\Gamma}_{max} \simeq -\frac{1}{\tau} + \frac{e^2\left(\omega_1-\omega_2\right)\left|\mathcal{E}_1\mathcal{E}_2\right|}{mE_0\left(\omega_1+\omega_2\right)\left|3\omega_2-\omega_1\right|} > 0 \quad . \tag{3.47}$$

There is no real divergence in Eqs. (3.46-3.47) in the limit $\omega_1 \to 3\omega_2$, since they have been derived under the assumption $|3\omega_2 - \omega_1| \gtrsim 1/\tau$.

Saturation of Parametric Resonance

As the threshold for parametric resonance is exceeded, the harmonics with frequency $(\omega_1+\omega_2)/2$ can no longer be considered as a perturbation, but rather have to be included into the equation of motion. In other words, we have to search for a solution of Eq. (3.18) in the form

$$\mathcal{P} = \mathcal{P}_1^+ \exp\left(i\omega_1 t\right) + \mathcal{P}_2^+ \exp\left(i\omega_2 t\right) + \mathcal{P}_3(t)\exp\left[i\left(\frac{\omega_1+\omega_2}{2}\right)t\right] \quad , \tag{3.48}$$

where $\mathcal{P}_3(t)$ is a slowly-varying function of time. Upon substituting this form into Eq. (3.18), we obtain the following coupled system of equations for $\mathcal{P}_3(t)$ and $\mathcal{P}_3^*(t)$

$$\begin{aligned}\frac{d\mathcal{P}_3}{dt} + \left[\frac{1}{\tau} + \frac{i\left(\omega_1+\omega_2-2\omega_c\right)}{2} + \frac{i\omega_c}{mE_0}\left(2|\mathcal{P}_1^+|^2 + 2|\mathcal{P}_2^+|^2 + |\mathcal{P}_3|^2\right)\right]\mathcal{P}_3 \\ = -\frac{2i\omega_c}{mE_0}\mathcal{P}_1^+\mathcal{P}_2^+\mathcal{P}_3^* \quad ,\end{aligned} \tag{3.49}$$

$$\begin{aligned}\frac{d\mathcal{P}_3^*}{dt} + \left[\frac{1}{\tau} - \frac{i\left(\omega_1+\omega_2-2\omega_c\right)}{2} - \frac{i\omega_c}{mE_0}\left(2|\mathcal{P}_1^+|^2 + 2|\mathcal{P}_2^+|^2 + |\mathcal{P}_3|^2\right)\right]\mathcal{P}_3^* \\ = \frac{2i\omega_c}{mE_0}\left(\mathcal{P}_1^+\mathcal{P}_2^+\right)^*\mathcal{P}_3 \quad .\end{aligned} \tag{3.50}$$

Saturated parametric instability can be reached by setting $d\mathcal{P}_3/dt = 0$ and $d\mathcal{P}_3^*/dt = 0$ in Eqs. (3.49) and (3.50), respectively. The result for $\mathcal{P}_3$ assumes its simplest form at the optimal magnetic field $\omega_c = \omega_c^{opt}$

$$|\mathcal{P}_3|(\omega_c^{opt}) = \left[|\mathcal{P}_1^+\mathcal{P}_2^+|^2 - \frac{4m^2E_0^2}{\left(\omega_1+\omega_2\right)^2\tau^2}\right]^{1/4} \quad . \tag{3.51}$$

From Eq. (3.51), we conclude that in the vicinity of the threshold, $|\mathcal{P}_3|$ increases as $\left(|\mathcal{E}_1\mathcal{E}_2| - |\mathcal{E}_1\mathcal{E}_2|_c\right)^{1/4} \propto \Gamma_{max}^{1/4}$. Well above the threshold it approaches the value $|\mathcal{P}_1^+\mathcal{P}_2^+|^{1/2}$. Thus, even upon saturation, the magnitude of the nonparabolicity-induced harmonics with frequency $(\omega_1+\omega_2)/2$ does not have a "back"-effect on the magnitudes (Eq. (3.36)) of the responses to the ac fields.

For magnetic fields in the vicinity of ω_c^{opt}, the saturation value $|\mathcal{P}_3|(\omega_c)$ is given by

$$\begin{aligned} |\mathcal{P}_3|(\omega_c) &= \left\{ \left[|\mathcal{P}_1^+\mathcal{P}_2^+|^2 - \frac{4m^2E_0^2}{(\omega_1+\omega_2)^2\tau^2} \right]^{1/2} - \frac{2mE_0|\omega_c-\omega_c^{opt}|}{(\omega_1+\omega_2)} \right\}^{1/2} \\ &\simeq \left[|\mathcal{P}_3|^2(\omega_c^{opt}) - \frac{2mE_0|\omega_c-\omega_c^{opt}|}{(\omega_1+\omega_2)} \right]^{1/2} . \end{aligned} \tag{3.52}$$

In contrast to $|\mathcal{P}_3|(\omega_c^{opt})$, the threshold behavior of $|\mathcal{P}_3|(\omega_c)$ is slower, namely $|\mathcal{P}_3|(\omega_c) \propto \left(|\mathcal{E}_1\mathcal{E}_2| - |\mathcal{E}_1\mathcal{E}_2|_c\right)^{1/2}$. In principle, one has to verify that the solutions Eqs. (3.51-3.52), which describe the saturated parametric resonance, are stable. This can be done by perturbing Eqs. (3.49-3.50) around the saturated solution. We find that the corresponding perturbations do indeed decay.

Implications for dc Transport

As demonstrated in the previous subsection, the parametric instability that develops in the case of two ac fields above a certain threshold results in the momentum component $\mathcal{P}_3 \exp\left[i\left(\omega_1+\omega_2\right)t/2\right]$, which well above the threshold has the magnitude $|\mathcal{P}_3| \simeq \sqrt{|\mathcal{P}_1||\mathcal{P}_2|}$. The important consequence of the developed parametric resonance is that the component $\mathcal{P}_3$ gives rise to new harmonics in the term $\propto |\mathcal{P}|^2\mathcal{P}$ in the equation of motion, Eq. (3.18). Of particular interest are the $\mathcal{P}_3$-induced terms

$$\left[\mathcal{P}_1^2\mathcal{P}_3^* + \mathcal{P}_1\mathcal{P}_2^*\mathcal{P}_3\right] \exp\left(i\frac{3\omega_1-\omega_2}{2}t\right) . \tag{3.53}$$

It is easy to see that, under the condition $\omega_2 \simeq 3\omega_1$, these terms act as an effective dc field, and thus generate low-frequency *circular* current even without dc drive. If the relation between the frequencies is precisely 1 : 3, then the magnetic field, at which the developed parametric instability would give rise to a quasistationary circular current distribution, can be determined from Eq. (3.42)

$$\omega_c \simeq 2\omega_1\left[1 + \frac{2e^2\left(\mathcal{E}_1^2+\mathcal{E}_2^2\right)}{mE_0\left(\omega_1-\omega_2\right)^2}\right] . \tag{3.54}$$

If the ratio ω_2/ω_1 is close, but not exactly 1 : 3, there still is a certain allowance, determined by Eq. (3.45), for the formation of the quasistationary current. The above effect of spontaneous formation of dc-like currents under irradiation is distinctively different from the formation of current domains when σ_d turns

negative under irradiation. First, the effect is specific to bichromatic irradiation. Second, it requires rather strict commensurability between the two frequencies, and, finally, it develops within a very narrow interval around a certain magnetic field.

3.3 Bichromatic Irradiation and Absolute Negative Conductivity

Bichromatic irradiation can be used to test the assumption that absolute negative local conductivity lies at the origin of the observed ZRS. Consider a system under the influence of two microwave fields of frequencies ω_1 and ω_2. We are then interested in the following scenario: Under monochromatic irradiation with frequency ω_1, the diagonal resistance R_1 is positive and no ZRS are observed as the measured resistance is $R_1^{\text{exp.}} > 0$, while under mononchromatic irradiation with frequency ω_2, the diagonal resistance R_2 assumes negative values and thus drives the system to the ZRS-producing instability with an experimentally measured resistance $R_2^{\text{exp.}} = 0$. What happens if one simultaneously illuminates the sample with both microwave fields?

In the case of bichromatic irradiation, the stability of the combined response to both microwave fields depends on the amplitude of the corresponding contributions, with R_1 driving the system in one and R_2 in the opposite direction. If the positive response dominates ($|R_1| > |R_2|$), the bichromatic resistance will be stable even though the response to the microwave field of frequency ω_2 alone would lead to an instability. The monochromatic resistance R_2 can then be extracted from the bichromatic resistance R_{12} via

$$R_2 = 2R_{12} - R_1 \quad , \tag{3.55}$$

where it has been assumed that the intensities of both fields are tuned such that their contribution to the total resistance is equal. Certainly, this relation is too simplistic to be exact, but nevertheless allows for a first estimate of the magnitude of R_2.

Bichromatic irradiation thus allows to extract the value of R_2 masked by the instability in the monochromatic case (through $R_2^{\text{exp.}} = 0$) and thus can be used as a probe for absolute negative resistance. A corresponding experiment recently has been carried out by Zudov and co-workers [38], who found evidence for absolute negative resistance by irradiating a symmetrically doped AlGaAs/GaAs/AlGaAs quantum well mono- and bichromatically with frequencies $f_1 = \omega_1/2\pi = 31$ GHz and $f_2 = \omega_2/2\pi = 47$ GHz, which, by their ratio of $2:3$ allows for multiple overlaps between microwave-induced features of the monochromatic responses. Results of this experiment are shown in Fig. 3.7. Shown in panels (a) and (b) are the monochromatic responses to microwaves of frequencies ω_1 and ω_2 and, in panel (c), the response to simultaneous irradiation with both frequencies. The dotted curve in panel (c) represents the average of the mononchromatic resistances presented in panels (a) and (b). It is obvious that the measured bichromatic resistance lies well below this average for most magnetic fields, indicating a negative contribution by one of the two frequencies

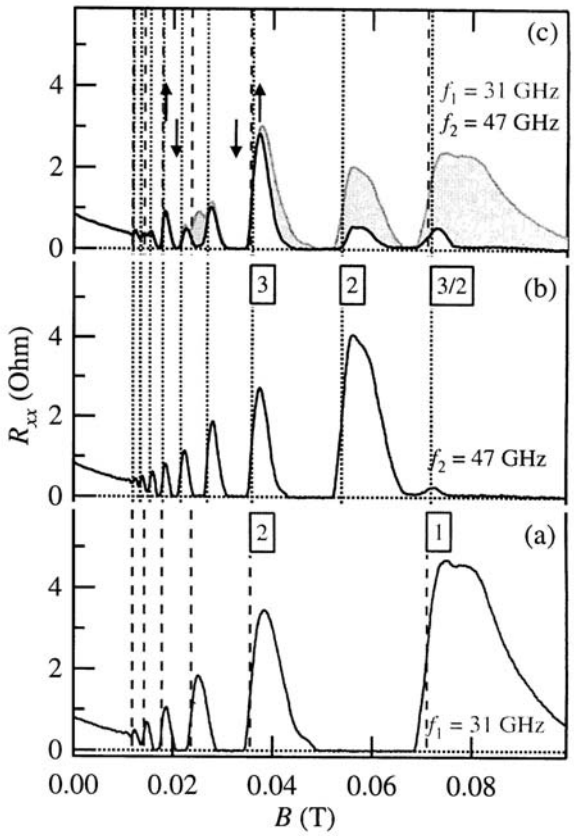

Figure 3.7: Results of the first experiment involving bichromatic irradiation [38]. Panels (a) and (b) show the longitudinal resistance R_{xx} under monochromatic irradiation with the individual microwave fields of frequencies f_1 and f_2 and panel (c) the resistance under bichromatic irradiation. Vertical lines mark the cyclotron harmonics as labeled by the boxed numbers. Wherever ZRS occur in the monochromatic cases (a)-(b), the total bichromatic resistance is reduced considerably with respect to the sum of the individual monochromatic resistances. This figure has been taken from Ref. [38].

and thus pointing towards the existence of absolute negative resistance. Wherever ZRS are present in the monochromatic cases, the bichromatic resistance is lowered considerably below the averaged value of the two mononchromatic resistances. This constitutes an important argument for the validity of the theoretical picture for the explanation of ZRS discussed in Chapter 2.

3.4 Discussion

In this chapter, we considered the problem of classical single electron motion in a magnetic field under simultaneous irradiation by two monochromatic fields. When the frequencies ω_1 and ω_2 differ only slightly, $|\omega_1 - \omega_2| \sim 1/\tau$, the effect of a weak nonparabolicity in the electron spectrum on the diagonal conductivity is qualitatively the same for monochromatic [59] as for bichromatic irradiation.

The main qualitative effect new to the bichromatic case is the emergence of parametric resonance at magnetic fields $\omega_c = (\omega_1 + \omega_2)/2$ and $\omega_c = |\omega_1 - \omega_2|/2$ when the detuning is strong, i.e. of the order of the cyclotron frequency. As discussed in detail in the introduction of this chapter, it is instructive to compare this effect with the parametric resonance of electrons in a magnetic field due to a weak time modulation of the field amplitude [60, 61, 62]. The latter effect, considered more than 20 years ago, has a transparent explanation: The modulation of the magnitude of a dc field with frequency $2\omega_c$ translates into a corresponding modulation of the cyclotron frequency, so that the equation of motion of the electron reduces to that for a harmonic oscillator with a weakly time-modulated eigenfrequency. The solution of this equation develops an instability if the frequency of the modulation is close to $2\omega_c$. For realistic magnetic field strengths, this condition on the modulation frequency of the magnetic field cannot be reached experimentally since the cyclotron frequency lies in the microwave range. It was proposed in Ref. [62] to use microwave illumination with frequency $2\omega_c$ to create a parametric resonance due to the *magnetic field* component of the pumping electromagnetic wave.

We have demonstrated in this chapter that two nonresonant ac sources can *enforce* a parametric resonance of the type considered in Refs. [60, 61, 62] *without* any time modulation of the dc magnetic field. Remarkably, the bichromatic-radiation-induced cyclotron resonance emerges due to the same nonparabolicity, Eq. (3.2), that played the role of a stabilizing factor in Refs. [60, 61, 62]. Roughly, the time modulation of ω_c in the dc field required in Refs. [60, 61, 62] for parametric resonance emerges from the "beatings" of the responses to the two ac signals. The nonparabolicity transforms these beatings into a modulation of the cyclotron frequency. Although the increment Γ for parametric resonance, induced by bichromatic irradiation, is proportional to the product $\mathcal{E}_1\mathcal{E}_2$ of the amplitudes of the two sources, while in Ref. [62] it was proportional to the *first power* of the magnetic component of the ac field, the "bichromatic" increment is much bigger. As demonstrated above, the bichromatic increment is $\Gamma \sim \omega_c \left(mc^2/E_0\right)\left(\mathcal{E}_1\mathcal{E}_2/B^2\right)$, which has to be compared to the increment $\Gamma \sim \omega_c \left(\mathcal{E}/B\right)$ of Ref. [62]. The ratio contains a small factor $(\mathcal{E}/B)$ which is offset by the huge factor $\left(mc^2/E_0\right)$.

Bichromatic irradiation can be used as a probe of the absolute negative longitudinal resistance believed to be the origin of the ZRS (see Chapter 2) by comparing the response of a system to bichromatic irradiation with the responses to the individual microwave fields. Very recently, this idea has been realized experimentally [38] and strong evidence for absolute negative resistance has been found.